Article

Not peer-reviewed version

Exploring Aggregation-Induced Emission in Anthracene-Naphthalene Derivatives for Selected Detection of Nitro Explosives

Sai Zhang * and Pincheng Wang

Posted Date: 18 December 2025

doi: 10.20944/preprints202512.1547.v1

Keywords: AIE; fluorescence; picric acid; sensing application

Article

Exploring Aggregation-Induced Emission in Anthracene-Naphthalene Derivatives for Selected Detection of Nitro Explosives

Sai Zhang,[1,*,#] and Pincheng Wang[2,#]

[1] School of Pharmacy, Changzhou University, Changzhou 213164, Jiangsu Province, China

[2] School of Environmental Science and Engineering, Changzhou University, Changzhou 213164, Jiangsu Province, China

* Correspondence: zhangsai@cczu.edu.cn

[#] These authors have equal contribution

Abstract

The detection of nitro explosives is critical for security and environmental monitoring. This study investigates the aggregation-induced emission (AIE) properties of anthracene and naphthalene derivatives, under varying water fractions between 0% and 70%. These compounds exhibit enhanced fluorescence due to AIE, making them suitable candidates for sensing applications. We demonstrate that nitro compounds, including o-nitroaniline, m-nitroaniline, p-nitroaniline, and picric acid can effectively quench these AIE-active derivatives. The quenching phenomenon reveals that the electron-withdrawing nature of the nitro groups significantly impacts the fluorescence intensity of the probes. This research highlights the potential of these anthracene derivatives as sensitive fluorescent probes for the selected detection of nitro explosives, paving the way for advancements in sensing technologies.

Keywords: AIE; fluorescence; picric acid; sensing application

1. Introduction

The detection of nitro explosives has become increasingly vital in the realms of security,[1] environmental monitoring,[2] and forensic science.[3] Nitro compounds, such as nitrobenzene, o-nitroaniline, m-nitroaniline, p-nitroaniline, and picric acid, are prevalent in military applications and industrial processes.[4]-[5] Their hazardous nature necessitates the development of effective and sensitive detection methods.[6]-[10] Traditional analytical techniques, while robust, often involve complex sample preparation and sophisticated instrumentation, which can hinder real-time analysis and field application.

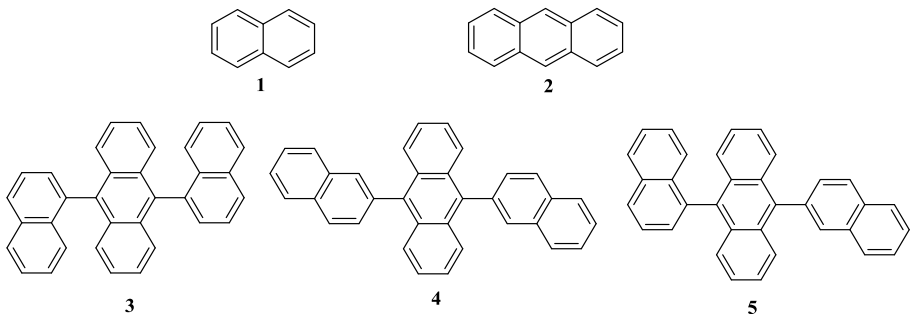

Figure 1. Selected Compounds **1**(naphthalene), **2**(anthracene), **3**(9,10-di(naphthalen-1-yl)anthracene), **4**(9,10-di(naphthalen-2-yl)anthracene), **5**(9-(naphthalen-1-yl)-10-(naphthalen-2-yl)anthracene).

 doi:10.20944/preprints202512.1547.v1

In recent years, fluorescence-based sensors have emerged as promising alternatives for the detection of nitro explosives.[11]-[15] These sensors utilize the unique optical properties of fluorescent materials, allowing for rapid and sensitive detection with minimal sample preparation. Among the various classes of fluorescent compounds, those exhibiting aggregation-induced emission (AIE) properties have garnered significant attention.[16]-[18] AIE refers to the phenomenon where certain compounds show enhanced fluorescence upon aggregation, in stark contrast to conventional fluorescent materials that typically quench in aggregated states.[19]-[21] Anthracene and naphthalene derivatives are fluorescence-active compounds that exhibit significant fluorescence modulation depending on their emission state.[22]-[23] This research has demonstrated that these compounds display pronounced AIE effects within a water fraction range of 0% to 70%. Within this range, the transition from a weakly emissive state to a highly emissive state occurs, making them particularly suitable for sensing applications. While anthracene and naphthalene exhibit intrinsic luminescence in organic solvents, their emission intensity is significantly enhanced upon aggregation due to restricted intramolecular motion, a hallmark of the AIE phenomenon.[19]-[21], [22]-[23] This aggregation-induced enhancement in fluorescence provides a robust platform for developing sensitive detection systems for nitro compounds. The ability to manipulate fluorescence intensity through changes in solvent composition provides a unique platform for developing sensitive detection systems for nitro compounds. Among the promising AIE-active derivatives, 9,10-di(naphthalen-1-yl)anthracene **3**, 9,10-di(naphthalen-2-yl)anthracene **4**, and 9-(naphthalen-1-yl)-10-(naphthalen-2-yl)anthracene **5** stand out due to their structural features and fluorescence properties. These compounds have shown potential as effective sensing agents, particularly in their ability to undergo fluorescence quenching in the presence of nitro compounds. The quenching mechanisms may involve electron transfer, energy transfer, or the formation of non-fluorescent complexes, which can be exploited to design sensitive detection systems. The interaction between AIE-active compounds and nitro explosives is particularly noteworthy. Nitro compounds possess electron-withdrawing nitro groups that can significantly influence the electronic properties of nearby fluorescent molecules, leading to a decrease in fluorescence intensity. This sensitivity to environmental changes positions AIE-active compounds as suitable candidates for detecting low concentrations of nitro explosives, which is essential for effective monitoring in practical applications.

In this study, we aim to investigate the quenching behavior of 9,10-di(naphthalen-1-yl)anthracene **3**, 9,10-di(naphthalen-2-yl)anthracene **4**, and 9-(naphthalen-1-yl)-10-(naphthalen-2-yl)anthracene **5** (Figure 1) in the presence of nitrobenzene, o-nitroaniline, m-nitroaniline, p-nitroaniline, and picric acid. We will explore the extent of fluorescence quenching and elucidate the underlying mechanisms responsible for this behavior. By understanding these interactions, we aim to establish the potential of these AIE-active compounds as fluorescent probes for the selected detection of nitro explosives, contributing to advancements in sensing technologies.

2. Aggregation phenomenon

The investigation of the ultraviolet (UV) absorption spectra of naphthalene and anthracene revealed intriguing insights into their aggregation behavior. Both naphthalene and anthracene displayed slight aggregation-induced absorbance, characterized by subtle shifts in their UV spectra as the water fraction increased. This phenomenon is indicative of the formation of an excimer or aggregate species, which can lead to changes in electronic transitions and, consequently, the absorbance characteristics.

In the UV spectrum of naphthalene, a relatively sharp absorption peak is observed (Figure 2A), corresponding to its π-π^* transitions. However, as the water fraction increases, a slight broadening of the absorption band and a tailing effect becomes evident. This tailing is likely due to aggregated species forming, which can absorb light at slightly different wavelengths than the monomeric form. The aggregation leads to a distribution of energy states, causing a shift in the absorption maximum and the appearance of a broader spectral profile.

 doi:10.20944/preprints202512.1547.v1

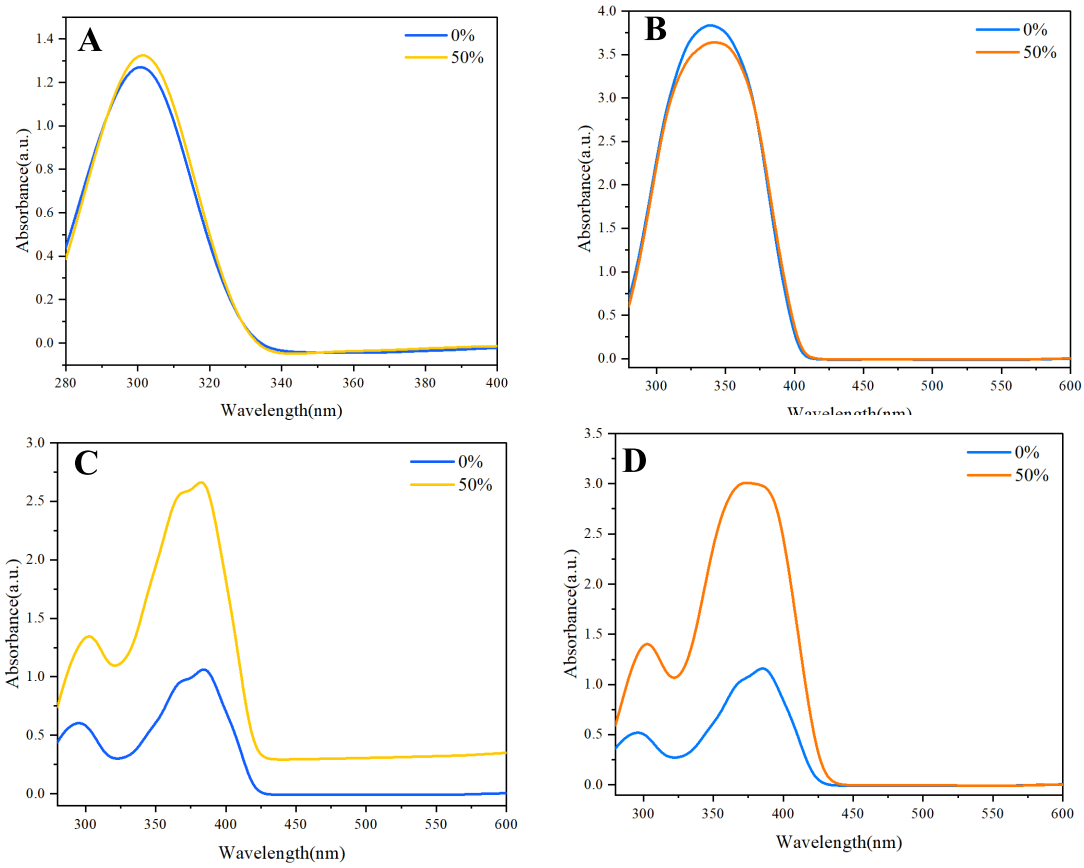

Figure 2. A. UV/vis absorption spectra of compound **1** in THF or THF/H_2O mixture; c = 0.01mg/mL. B.UV/vis absorption spectra of compound **2** in THF or THF/H_2O mixture; c = 0.01mg/mL. C.UV/vis absorption spectra of compound **3** in THF or THF/H_2O mixture; c = 0.01mg/mL. D.UV/vis absorption spectra of compound **5** in THF or THF/H_2O mixture; c = 0.01 mg/mL.

Similarly, anthracene exhibited a comparable trend, albeit with more pronounced effects (Figure 2B). The absorption spectrum of anthracene also showed a clear peak associated with its π-π* transitions. However, the aggregation-induced effects are not as noticeable as naphthalene, but there is broader absorption band and significant tailing observed as the water fraction increased. The aggregation of anthracene molecules can result in the formation of excimers, which are well-known to exhibit distinct absorption characteristics compared to their monomeric counterparts. This excimer formation is attributed to the close proximity of anthracene molecules, allowing for intermolecular interactions that alter their electronic properties.

In contrast, when examining the UV spectra of the synthesized derivatives—9,10-di(naphthalen-1-yl)anthracene **3** and 9-(naphthalen-1-yl)-10-(naphthalen-2-yl)anthracene **5**, the phenomenon of aggregation was significantly more pronounced (Figure 2C and Figure 2D). The absorption spectra of compound **4** were omitted from Figure 2 as it showed no notable tailing or intensity changes with water fraction, indicating negligible aggregation behavior compared to derivatives 3 and 5. The UV absorption spectra of these compounds **1**, **2**, **3**, and **5** displayed markedly increased absorbance and more extensive tailing, suggesting a higher propensity for aggregation compared to naphthalene and anthracene alone. The UV spectra exhibited broader absorption bands, indicating the presence of multiple electronic states due to aggregation. This behavior underscores the importance of molecular design in influencing the optical properties of organic compounds. The UV spectral analysis of naphthalene, anthracene, and their derivatives reveals significant insights into the aggregation-induced absorbance and tailing phenomenon. The slight aggregation observed in naphthalene and anthracene becomes markedly pronounced in their derivatives, highlighting the influence of

 doi:10.20944/preprints202512.1547.v1

molecular structure on aggregation behavior. The observed spectral broadening in the UV and photoluminescence spectra of naphthalene, anthracene, and their derivatives can be attributed to aggregation effects rather than instrumental limitations. Instrumental factors, such as slit width or detector resolution, typically produce consistent broadening across all samples, which was not observed here. Instead, the broadening and tailing effects were concentration- and solvent-dependent, aligning with the formation of aggregates or excimers. For instance, the broadening in naphthalene and anthracene spectra at higher water fractions (Figure 2A, 2B) reflects the distribution of electronic states due to intermolecular interactions in aggregated species. This is further supported by the derivatives (e.g., compounds 3 and 5), where structural modifications enhanced aggregation, leading to more pronounced spectral changes (Figure 2C, 2D). The absence of such effects in compound 4 underscores the role of molecular design. These findings are consistent with AIE literature, where aggregation restricts intramolecular motion, altering emission profiles. Thus, the broadening is a intrinsic property of the aggregated states, providing a clear distinction from instrumental artifacts.

The absorption spectra were measured at 50% water content due to experimental constraints at higher water fractions (e.g., 70%), where excessive scattering and precipitation interfered with spectral clarity. Despite this, the 50% condition provided sufficient aggregation to observe meaningful absorbance shifts, aligning with the AIE trends observed in photoluminescence studies at higher water fractions.

Having identified the aggregation behavior through UV spectra, the subsequent step involves measuring photoluminescence to assess the limitations imposed by aggregation. In the photoluminescence measurements, naphthalene and anthracene exhibited a pronounced aggregation-induced emission (AIE) phenomenon as the water fraction increased from 0% to 70%. Initially, both compounds demonstrated weak emission in pure organic solvents due to non-radiative decay processes prevalent in their dissolved states. However, as the water fraction was gradually increased, a significant enhancement in luminescence was observed, indicative of AIE (Figure 3A and Figure 3B). This enhancement can be attributed to the aggregation of the naphthalene and anthracene molecules, driven by hydrophobic interactions in the presence of water. At approximately 70% water content, the emission intensity peaked, suggesting an optimal aggregation state that effectively restricted intramolecular motion and minimized energy loss through non-radiative pathways. Beyond this threshold, further increases in water content led to a decline in luminescence, likely due to excessive aggregation or solubility issues. These results highlight the critical role of solvent composition in modulating the photophysical properties of naphthalene and anthracene (Figure 3A and Figure 3B). The observed bathochromic shift of approximately 5-10 nm in the emission maximum of anthracene (**2**) as the water fraction increases from 0-50% to 60-90% is indicative of aggregate formation. This redshift is characteristic of the formation of J-aggregates or excimers, where the close packing of molecules in the aggregated state results in a lower energy excited state. The more pronounced shift at higher water fractions (60-90%) suggests the formation of larger or more ordered aggregates, which exhibit stronger intermolecular interactions and thus a greater stabilization of the excited state compared to the initial aggregates formed at lower water content.

In exploring the aggregation-induced emission (AIE) characteristics of naphthalene and anthracene, we extended our investigation to three derivatives: 9,10-di(naphthalen-1-yl)anthracene **3**, 9,10-di(naphthalen-2-yl)anthracene **4**, and 9-(naphthalen-1-yl)-10-(naphthalen-2-yl)anthracene **5**. Unlike the pronounced AIE observed in naphthalene and anthracene, the derivatives displayed only a slight AIE phenomenon when the water fraction ranged between 0% and 50% (**3** in Figure 3C, **4** in Figure 3D, and **5** in Figure 3E). This modest enhancement in fluorescence intensity can be attributed to the limited aggregation of the molecules, which, while promoting some degree of restriction on intramolecular motion, did not reach the optimal conditions for significant AIE. As the water fraction continued to rise beyond 50%, a noticeable quenching of fluorescence intensity was observed, culminating in a significant decrease as the water fraction approached 90% (**3** in Figure 3C, **4** in Figure 3D, and **5** in Figure 3E). This quenching could be linked to excessive aggregation and potential

 doi:10.20944/preprints202512.1547.v1

solubility issues that disrupt the compact, rigid structure necessary for efficient radiative transitions. The observed slight AIE phenomenon in these derivatives suggests a scientific relationship with the AIE behavior of naphthalene and anthracene. While the derivatives exhibit reduced AIE efficiency, their photophysical properties still reflect the underlying principles of AIE, indicating that the structural modifications imparted by the naphthalene-anthracene combination influence their aggregation behavior and emission characteristics. The luminescence spectra of naphthalene and anthracene in THF/water mixtures exhibit broadened emission profiles, which may arise from the formation of aggregates or excimers under high water fractions. While literature reports distinct emission maxima for these compounds in monomeric form (e.g., naphthalene at 321, 334 nm and anthracene at 375, 396, 420 nm in pure solvents), the observed spectral similarity in our study likely reflects the dominant contribution of aggregated species under AIE conditions. This behavior aligns with previous studies on AIE-active systems, where aggregation can lead to significant spectral shifts and broadening.[19]-[21] Figure 3 shows that derivatives 3-5 exhibit minimal emission enhancement ($\leqslant$10%) within the 0 – 50% water fraction range, within experimental error margins ($\pm$3%). This suggests their AIE activity is significantly weaker compared to 1-2, likely due to structural constraints limiting aggregation-induced rigidification. The observed trends align with their modest spectral shifts in UV studies (Figure 2).

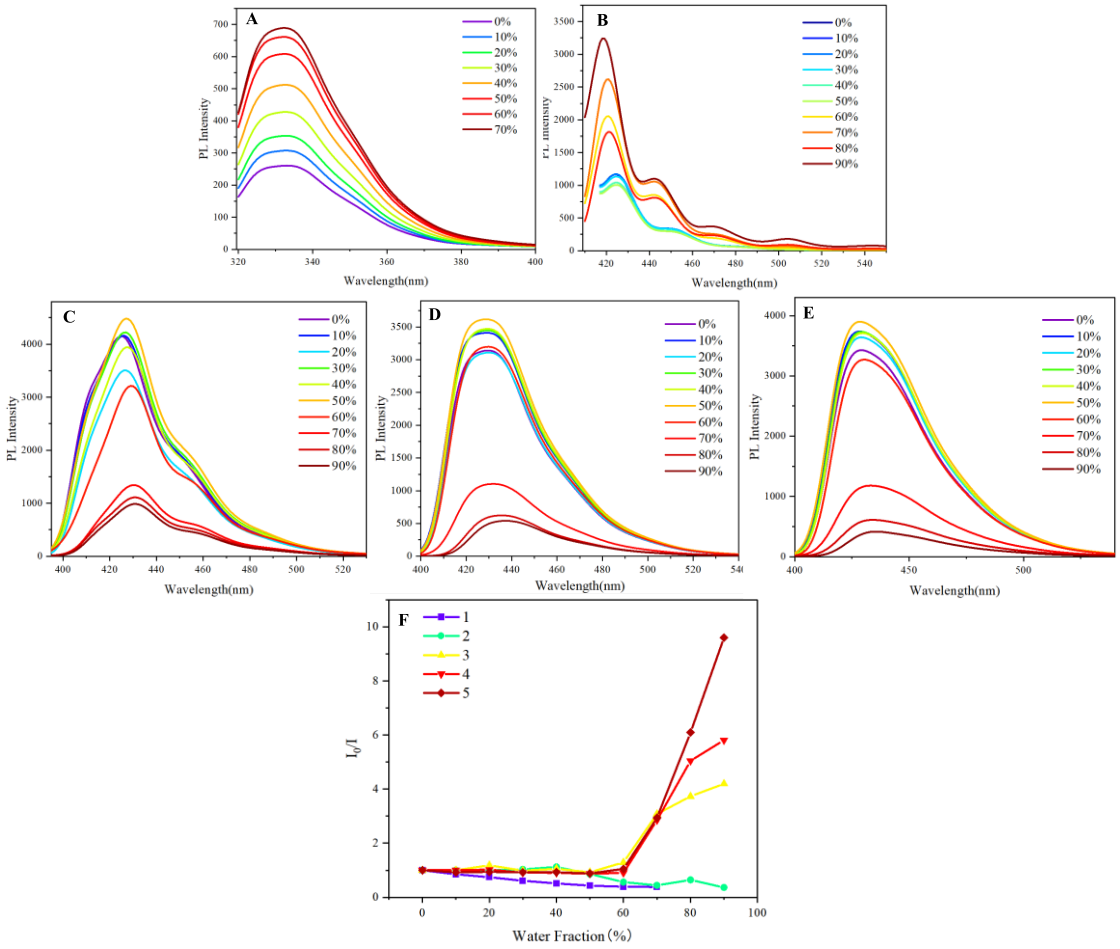

Figure 3. 1 (A), **2** (B), **3** (C), **4** (D), **5** (E) in THF/H2O mixture with different water fractions. Concentration: 0.05 mg/mL. Excitation wavelength: of **1-5**: 311 nm. F. Stern-Volmer plots of I_0/I vs. water fraction for **1-5.**

 doi:10.20944/preprints202512.1547.v1

3. Detection of Nitro Explosives

Recent advancements in photoluminescent materials have highlighted the potential of naphthalene-anthracene derivatives for detecting nitro explosives.[24]-[26] We investigated compounds 9,10-di(naphthalen-1-yl)anthracene **3**, 9,10-di(naphthalen-2-yl)anthracene **4**, and 9-(naphthalen-1-yl)-10-(naphthalen-2-yl)anthracene **5**. These derivatives exhibited notable changes in their fluorescence properties upon exposure to nitro compounds. The observed photoluminescence quenching suggests a strong interaction between the nitro explosives and the sensing materials, indicating their potential as effective sensors for security applications.

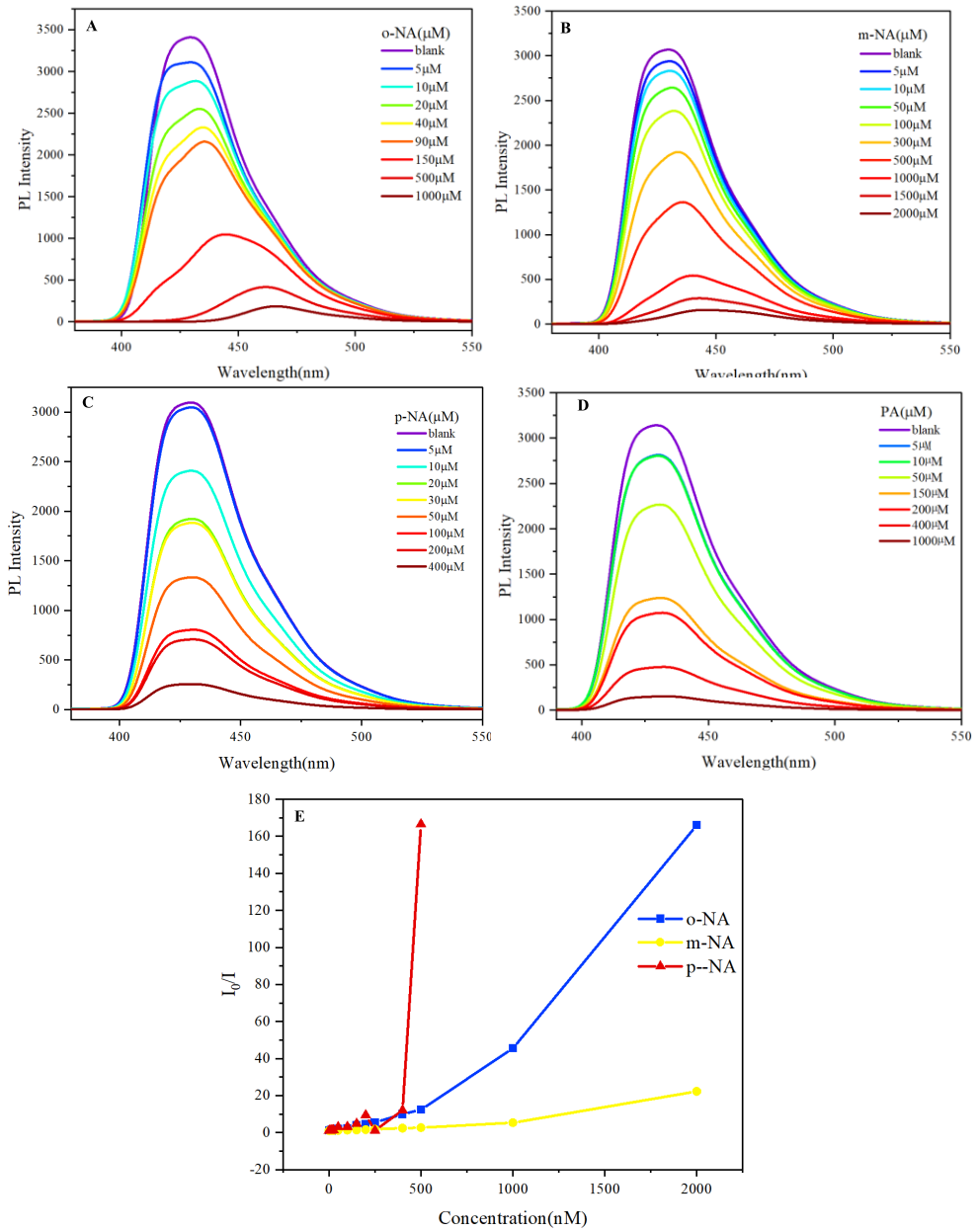

Figure 4. A-D. Fluorescence emission response of **3** on gradual addition of o-NA, m-NA, p-NA, and PA. Concentration of **3**: 0.05mg/mL(110μM) . Excitation wavelength: 311nm. Solvent: THF. E. Stern-Volmer plots of I_0/I vs. Concentration of Nitro-explosive(o-NA, m-NA and p-NA) in solution of compound **3**.

The photoluminescent properties of 9,10-di(naphthalen-1-yl)anthracene **3** were systematically investigated for the potential application in detecting nitroaniline derivatives and picric acid. The fluorescence response of this compound was assessed as the concentration of o-nitroaniline was

 doi:10.20944/preprints202512.1547.v1

varied from 5 μM to 2000 μM (Figure 4A). Notably, a complete quenching of fluorescence was observed at the highest concentration, indicating a strong interaction between the nitroaniline and the photoluminescent material. This phenomenon suggests that the quenching is likely due to non-radiative energy transfer processes facilitated by the electron-deficient nature of the nitro group. Similarly, the detection of m-nitroaniline exhibited a comparable trend, where an increase in concentration resulted in significant fluorescence quenching (Figure 4B). This consistent behavior across both o-nitroaniline and m-nitroaniline highlights the effectiveness of 9,10-di(naphthalen-1-yl)anthracene **3** as a sensing material for nitro compounds, underscoring its potential for practical applications in explosive detection. In contrast, the detection of p-nitroaniline revealed a notably enhanced quenching efficiency (Figure 4C). The fluorescence of 9,10-di(naphthalen-1-yl)anthracene was completely quenched at a concentration of only 500 μM. This increased sensitivity could be attributed to the spatial orientation and electronic interactions between the p-nitroaniline and the anthracene derivative, suggesting that the molecular structure of the nitro compound plays a crucial role in the quenching mechanism. Furthermore, when assessing picric acid, the sensitivity of 9,10-di(naphthalen-1-yl)anthracene **3** was significantly superior compared to the previously tested nitroanilines. Complete fluorescence quenching was achieved at a concentration of 1500 μM (Figure 4D). The pronounced quenching effect observed with picric acid indicates a robust interaction, likely due to the presence of multiple nitro groups that enhance the electron-withdrawing capacity, thereby facilitating more efficient energy transfer processes. The Stern-Volmer analysis (Figure 4E) reveals distinct quenching mechanisms for the nitro compounds. Linear plots for o-NA, m-NA, and p-NA are consistent with dynamic quenching, where diffusion-controlled collisions between the excited-state probe and nitro analytes dominate. The higher value for p-NA reflects its superior electron-withdrawing capability due to para-substitution, which enhances photoinduced electron transfer (PET). For PA, the upward-curving Stern-Volmer plot suggests additional static quenching via ground-state complexation, driven by its three nitro groups(Figure S2). This dual mechanism aligns with the probe's exceptional sensitivity to PA, achieving complete quenching at 100 μM. The observed quenching at sub-stoichiometric analyte concentrations underscores the efficiency of PET, wherein the nitro groups act as electron sinks, non-radiatively deactivating the excited state of the anthracene-naphthalene derivatives.

The photoluminescent properties of 9,10-di(naphthalen-2-yl)anthracene **4** were evaluated for its efficacy in detecting various nitro compounds, specifically o-nitroaniline, m-nitroaniline, p-nitroaniline, and picric acid (Figure S1). The fluorescence response of this compound exhibited trends analogous to those observed with 9,10-di(naphthalen-1-yl)anthracene **3**, indicating that structural modifications in the naphthalene substituents do not significantly alter the quenching behavior against these nitro explosives.

As the concentration of o-nitroaniline increased, a pronounced quenching of fluorescence was recorded, culminating in complete quenching at elevated concentrations (Figure S1A). The detection of m-nitroaniline also demonstrated significant fluorescence quenching, reinforcing the compound's capability to serve as a reliable sensor for nitroanilines (Figure S1B). The response to p-nitroaniline was particularly noteworthy, as complete quenching occurred at lower concentrations compared to o- and m-nitroaniline (Figure S1C). Moreover, the responsiveness of 9,10-di(naphthalen-2-yl)anthracene to picric acid paralleled that of the other nitro compounds (Figure S1D), with substantial quenching observed at relatively high concentrations the photoluminescent properties of 9-(naphthalen-1-yl)-10-(naphthalen-2-yl)anthracene **5** were investigated for the detection of nitro compounds, specifically o-nitroaniline, m-nitroaniline, p-nitroaniline, and picric acid. The fluorescence response of this compound exhibited behavior analogous to that observed with both 9,10-di(naphthalen-1-yl)anthracene **3** and 9,10-di(naphthalen-2-yl)anthracene **4**. As the concentration of each nitro compound increased, significant quenching of fluorescence was noted, culminating in complete quenching at higher concentrations (Figure 5). This consistent trend across the different naphthalene-substituted anthracenes suggests that the structural variations do not substantially impact the quenching efficiency. The pronounced quenching observed for p-

 doi:10.20944/preprints202512.1547.v1

nitroaniline at lower concentrations further emphasizes the enhanced sensitivity of these compounds towards specific nitro groups. Additionally, the effective quenching response to picric acid indicates the potential of these photoluminescent materials for practical applications in explosive detection.

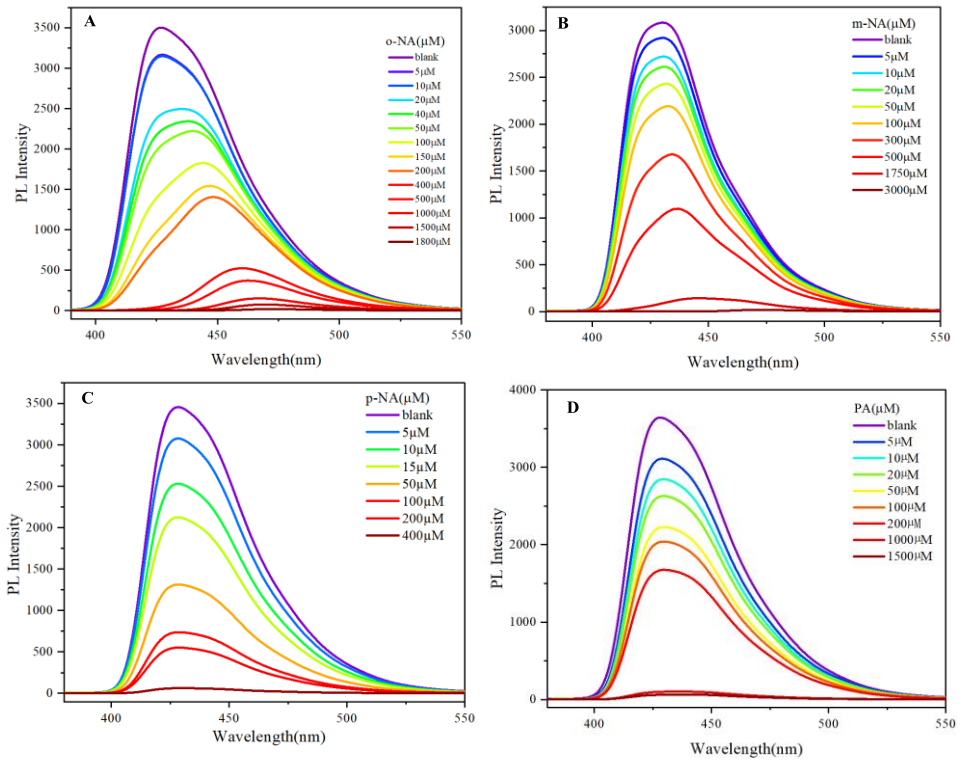

Figure 5. A-D. Fluorescence emission response of **5** on gradual addition of o-NA, m-NA, p-NA, and PA. Concentration of **5**: 110μM . Excitation wavelength: 330nm. Solvent: THF.

4. RGB Analysis

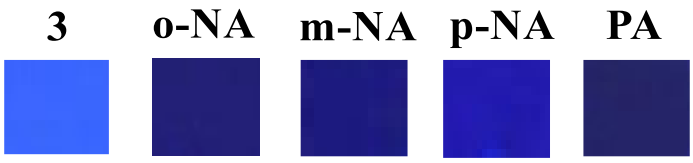

Figure 6. RGB Analysis of compound **3** mixed with o-NA, m-NA, p-NA and PA. Inert: 100mM for compound 3, and o-NA, m-NA, p-NA,PA is 500μM.

RGB (Red, Green, Blue) analysis is a powerful technique for quantifying colorimetric changes in luminescent materials upon interaction with nitro explosives. This method decomposes color into its primary components, enabling precise discrimination of analytes based on their unique spectral signatures. For this study, RGB analysis was performed on compound 3 in tetrahydrofuran (THF) to evaluate its fluorescence response to nitro explosives, including o-nitroaniline (o-NA), m-nitroaniline (m-NA), p-nitroaniline (p-NA), and picric acid (PA). THF was chosen as the solvent for RGB analysis due to its ability to dissolve both the anthracene-naphthalene derivatives and nitro compounds uniformly, ensuring homogeneous mixing and consistent fluorescence measurements. THF also minimizes scattering interference, which is critical for accurate RGB quantification. The concentration of compound 3 was fixed at 100 μM, while nitro analytes were tested at 500 μM. This ratio (1:5 probe-

 doi:10.20944/preprints202512.1547.v1

to-analyte) was selected based on preliminary titration experiments (Figures 4–5), which showed that 500 μM of nitro compounds induced near-complete fluorescence quenching while avoiding saturation or precipitation. This concentration range optimizes sensitivity while maintaining linearity in the RGB response.

5. Conclusion

This study demonstrates the potential of anthracene and naphthalene derivatives (compounds 3, 4, and 5) as effective fluorescent probes for detecting nitro explosives. The aggregation-induced emission (AIE) phenomenon observed at water fractions between 0% and 50% enhances their fluorescence properties, making them suitable for sensing applications. Systematic titration experiments revealed significant fluorescence quenching upon exposure to nitroanilines (o-nitroaniline, m-nitroaniline, and p-nitroaniline) and picric acid, highlighting their sensitivity to nitro compounds.

The quenching mechanisms are attributed to the electron-withdrawing nature of nitro groups, which facilitate efficient energy or electron transfer. The derivatives exhibited pronounced responses, particularly to p-nitroaniline and picric acid, suggesting their utility in practical detection systems. RGB analysis further validated the fluorescence changes, providing a rapid and interpretable method for nitro compound identification.

These findings underscore the promise of anthracene-naphthalene derivatives as robust sensors for nitro explosives. Future work will focus on optimizing these probes for real-world applications in security and environmental monitoring, as well as exploring structural modifications to enhance their performance. This research contributes to the advancement of fluorescence-based sensing technologies for explosive detection.

6. Chemicals and Instruments

Chemicals: Naphthalene (1), anthracene (2), 9,10-di(naphthalen-1-yl)anthracene (3), 9,10-di(naphthalen-2-yl)anthracene (4), and 9-(naphthalen-1-yl)-10-(naphthalen-2-yl)anthracene (5) were purchased from Energy Chemical Co. Ltd. (Shanghai, China). Tetrahydrofuran (THF, HPLC grade) was used as the primary solvent for sample preparation. Nitro compounds, including o-nitroaniline (o-NA), m-nitroaniline (m-NA), p-nitroaniline (p-NA), and picric acid (PA), were obtained from Sigma-Aldrich and used without further purification.

Sample Preparation: Stock solutions of compounds **1–5** (0.01 mM) were prepared by dissolving the solids in THF. For aggregation studies, THF/water mixtures with varying water fractions (0–90% v/v) were prepared by adding deionized water to the THF stock solutions under vigorous stirring. Nitro compound solutions (5–2000 μM) were prepared in THF for quenching experiments. All solutions were sonicated for 10 minutes to ensure homogeneity and stored in amber vials to prevent photodegradation.

Instruments and Measurements:

UV-visible absorption spectra were recorded using a Shanghai Lengguang 759S spectrometer with a 1 cm quartz cuvette, scanning from 200 to 600 nm. Photoluminescence (PL) spectra were acquired on a Shanghai Lengguang F98 spectrometer equipped with a 150 W xenon lamp as the excitation source. For PL measurements, the excitation wavelength was set to 365 nm for compounds 1–5, with emission recorded from 380 to 650 nm. Slit widths for excitation and emission were fixed at 5 nm, and each spectrum was averaged over three scans to minimize noise.

Experimental Procedure of Detecting Nitro-explosive

Aggregation Studies: PL spectra of compounds 1–5 were measured in THF/water mixtures (0–90% water fraction) at room temperature.

 doi:10.20944/preprints202512.1547.v1

Quenching Experiments: Aliquots of nitro compound solutions (o-NA, m-NA, p-NA, or PA) were titrated into a fixed concentration (0.01 mM) of the probe solution (compounds 3–5 in 50% THF/water). After each addition, the mixture was equilibrated for 2 minutes before recording the PL intensity at the emission maximum.

Error Margins and Reproducibility

Concentrations were calculated using a calibrated micropipette (error margin: ±0.5%). Each measurement was repeated in triplicate, and the standard deviation of PL intensity was <3%. The detection limit (LOD) for nitro compounds was calculated as 3σ/slope, where σ is the standard deviation of blank measurements.

Experimental Details of RGB analysis

Sample Preparation: A stock solution of **3** (100 μM in THF) was mixed with aliquots of nitro compounds (500 μM in THF) in amber vials to prevent photodegradation. Solutions were sonicated for 10 minutes to ensure uniformity and equilibrated for 2 minutes before imaging.

Image Acquisition and Processing: Fluorescence images were captured under UV excitation (330 nm) using a standardized imaging setup with fixed exposure and white-balance settings.

RGB values were extracted from the emission spectra using ImageJ software, with background subtraction to isolate analyte-specific changes.

Colorimetric Interpretation: Compound 3 exhibited a dodger blue emission (dominant blue channel) in THF.

Upon addition of o-NA or m-NA, the color shifted to midnight blue (reduced blue/green intensity), reflecting fluorescence quenching via electron transfer. p-NA induced an indanthrene blue shift, suggesting stronger electronic interaction due to its para-substituted nitro group. PA yielded a slate color (balanced RGB reduction), consistent with its multi-nitro quenching efficiency (Figure 6).

Rationale for Conditions: The THF solvent system ensures compatibility with the hydrophobic aggregation behavior of **3**, while the 500 μM analyte concentration aligns with the dynamic range of the probe's quenching response. This approach balances signal-to-noise ratio with practical detection limits, as corroborated by the photoluminescence titration data (Figures 4–5). The RGB methodology thus provides a rapid, visually interpretable complement to spectral analysis, suitable for field applications.

References

1. D. S. Edwards, L. McMenemy, S. A. Stapley, H. D. L. Patel, J. C. Clasper, *Injury* **2016**, *47*, 646–652.
2. R. Sawant, S. Chakraborty, A. Papalkar, A. Awale, A. Chaskar, *Mater. Today Chem.* **2024**, *37*, 101983.
3. H. A. Yu, D. A. DeTata, S. W. Lewis, D. S. Silvester, *Trends Analyt. Chem.* **2017**, *97*, 374–384.
4. K. Zalewski, Z. Chyłek, W. A. Trzciński, *Polymers (Basel)* **2021**, *13*, 1080.
5. R. G. Ewing, D. A. Atkinson, G. A. Eiceman, G. J. Ewing, *Talanta* **2001**, *54*, 515–529.
6. Z.-D. Yu, J.-Y. Cao, H.-L. Li, G. Yang, W.-X. Zhao, C.-Z. Wang, S.-H. Chen, M. R. J. Elsegood, C. Redshaw, T. Yamato, *J. Lumin.* **2023**, *253*, 119439.
7. J.-Y. Cao, Z.-D. Yu, G. Yang, X.-C. Wang, L. Jiang, X. Wang, W.-X. Zhao, S.-H. Chen, C. Redshaw, C.-Z. Wang, T. Yamato, *J. Mol. Struct.* **2023**, *1285*, 135490.
8. A. Deshmukh, S. Bandyopadhyay, A. James, A. Patra, *J. Mater. Chem. C Mater. Opt. Electron. Devices* **2016**, *4*, 4427–4433.
9. S. Li, W. Liu, X. Song, C.-Z. Wang, C. Redshaw, X. Feng, *New J Chem* **2023**, DOI 10.1039/d3nj04102f.
10. H.-L. Li, J.-Y. Cao, Z.-D. Yu, G. Yang, Z.-M. Xue, C.-Z. Wang, W.-X. Zhao, Y. Zhao, C. Redshaw, T. Yamato, *Mater. Chem. Front.* **2023**, *7*, 3365–3372.
11. W. Liu, J. Qiao, J. Gu, Y. Liu, *Inorg. Chem.* **2023**, *62*, 1272–1278.
12. T. Ouyang, X. Guo, Q. Cui, W. Zhang, W. Dong, T. Fei, *Chemosensors (Basel)* **2022**, *10*, 366.
13. L.-L. Zhou, M. Li, H.-Y. Lu, C.-F. Chen, *Polym. Chem.* **2016**, *7*, 310–318.

 doi:10.20944/preprints202512.1547.v1

14. A. Natori, Y. Sanada, S. Sugahara, S. Nohara, Y. Seike, Y. Senga, *Mar. Chem.* **2024**, *259*, 104353.
15. M. Wu, X. Huang, L. Feng, Y. Sun, Y. Lu, L. Hu, S. Tian, T. She, F. Shen, S. Deng, D. Fang, *Water Res.* **2024**, 122582..
16. B. Dey, S. Ghosh, C. Charan Malakar, A. Kumar Atta, *Microchem. J.* **2024**, *200*, 110486.
17. R. Hu, A. Qin, B. Z. Tang, *Prog. Polym. Sci.* **2020**, *100*, 101176.
18. Q. Xia, A. Qin, B. Z. Tang, *J. Nanopart. Res.* **2023**, *25*, DOI 10.1007/s11051-022-05657-3.
19. J. Luo, Z. Xie, J. W. Y. Lam, L. Cheng, B. Z. Tang, H. Chen, C. Qiu, H. S. Kwok, X. Zhan, Y. Liu, D. Zhu, *Chem. Commun. (Camb.)* **2001**, 1740–1741.
20. J. Chen, B. Xu, X. Ouyang, B. Z. Tang, Y. Cao, *J. Phys. Chem. A* **2004**, *108*, 7522–7526..
21. Y. Hong, J. W. Y. Lam, B. Z. Tang, *Chem. Commun. (Camb.)* **2009**, 4332..
22. M. Tonga, *J. Photochem. Photobiol. A Chem.* **2021**, *412*, 113247.
23. S. Sasaki, S. Suzuki, W. M. C. Sameera, K. Igawa, K. Morokuma, G.-I. Konishi, *J. Am. Chem. Soc.* **2016**, *138*, 8194–8206.
24. Gupta, A.; Kaur, S.; Singh, H.; Garg, S.; Kumar, A.; Malhotra, E. Quantum Dots: A Tool for the Detection of Explosives/Nitro Derivatives. *Anal. Methods* **2023**, *15* (46), 6362–6376.
25. An, J. M.; Lim, Y. J.; Yeo, S. G.; Kim, Y. H.; Kim, D. Recent Advances of Nitrobenzoselenadiazole for Imaging and Therapy. *ACS Sens.* **2025**, *10* (3), 1709–1721.
26. Kosgei, G. K.; Fernando, P. U. A. I. Recent Advances in Fluorescent Based Chemical Probes for the Detection of Perchlorate Ions. *Crit. Rev. Anal. Chem.* **2025**, 1–25.